

AD-A066 131

MISSION RESEARCH CORP SANTA BARBARA CALIF

F/6 20/3

ON THE LIMITS OF APPLICABILITY OF THE SPACE-CHARGE-LIMITED P-DO--ETC(U)

JUN 78 R STETTNER

DNA001-77-C-0009

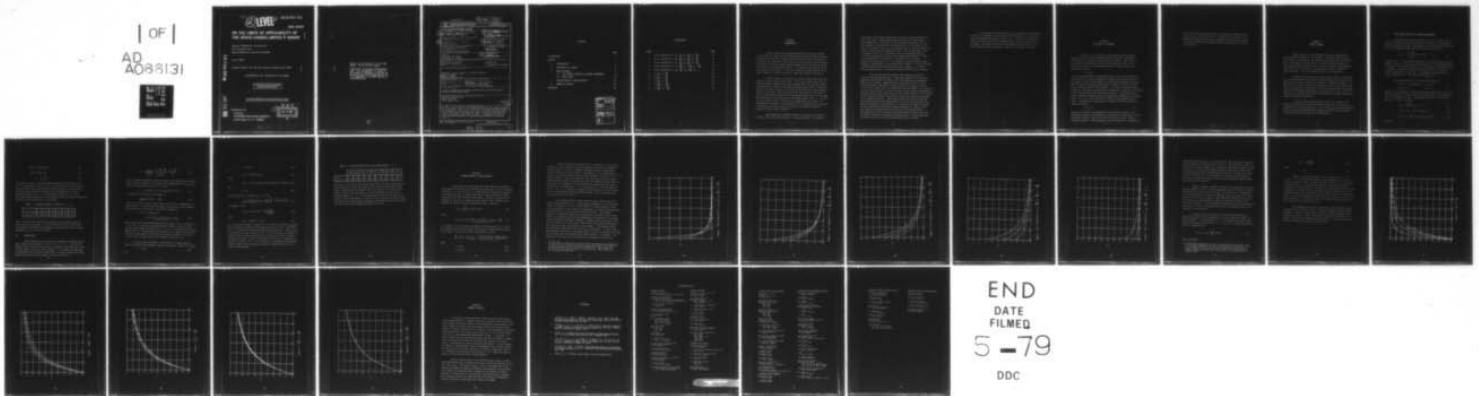
UNCLASSIFIED

MRC-N-348

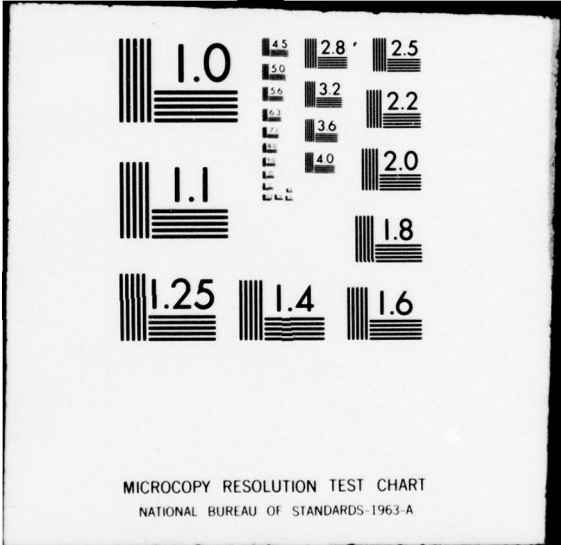
DNA-4630T

NL

1 OF 1
AD A066131
131



END
DATE
FILMED
5-79
DDC



12 LEVEL III
SC

AD-E300 464

DNA 4630T

ON THE LIMITS OF APPLICABILITY OF THE SPACE-CHARGE-LIMITED P DRIVER

Mission Research Corporation
P.O. Drawer 719
Santa Barbara, California 93102

June 1978

Topical Report for Period January 1978—June 1978

CONTRACT No. DNA 001-77-C-0009

APPROVED FOR PUBLIC RELEASE;
DISTRIBUTION UNLIMITED.

THIS WORK SPONSORED BY THE DEFENSE NUCLEAR AGENCY
UNDER RDT&E RMSS CODE B323077464 R99QAXEE50207 H2590D.

Prepared for
Director
DEFENSE NUCLEAR AGENCY
Washington, D. C. 20305

DDC
RECEIVED
MAR 22 1979
B

AD A0 661 31

DDC FILE COPY

79 02 05 008

Destroy this report when it is no longer
needed. Do not return to sender.

PLEASE NOTIFY THE DEFENSE NUCLEAR AGENCY,
ATTN: TISI, WASHINGTON, D.C. 20305, IF
YOUR ADDRESS IS INCORRECT, IF YOU WISH TO
BE DELETED FROM THE DISTRIBUTION LIST, OR
IF THE ADDRESSEE IS NO LONGER EMPLOYED BY
YOUR ORGANIZATION.



UNCLASSIFIED

18 DNA, SBIE

SECURITY CLASSIFICATION OF THIS PAGE (When Data Entered)

19 REPORT DOCUMENTATION PAGE		READ INSTRUCTIONS BEFORE COMPLETING FORM	
1. REPORT NUMBER DNA 4630T, AD-E 300 464	2. GOVT ACCESSION NO.	3. RECIPIENT'S CATALOG NUMBER	
4. TITLE (and Subtitle) ON THE LIMITS OF APPLICABILITY OF THE SPACE-CHARGE-LIMITED DRIVER.		5. TYPE OF REPORT & PERIOD COVERED Topical Report for Period Jan 98 - Jun 78	
7. AUTHOR(s) Roger Stettner		6. PERFORMING ORG. REPORT NUMBER MRC-N-348	
9. PERFORMING ORGANIZATION NAME AND ADDRESS Mission Research Corporation P.O. Drawer 719 Santa Barbara, California 93102		8. CONTRACT OR GRANT NUMBER(s) DNA 001-77-C-0009	
11. CONTROLLING OFFICE NAME AND ADDRESS Director Defense Nuclear Agency Washington, D.C. 20305		10. PROGRAM ELEMENT, PROJECT, TASK AREA & WORK UNIT NUMBERS NWED Subtask R99QAXEE502-07	
14. MONITORING AGENCY NAME & ADDRESS (if different from Controlling Office) R99QAXE		12. REPORT DATE June 1978	
16. DISTRIBUTION STATEMENT (of this Report) Approved for public release; distribution unlimited.		13. NUMBER OF PAGES 36	
17. DISTRIBUTION STATEMENT (of the abstract entered in Block 20, if different from Report) 35 p		15. SECURITY CLASS (of this report) UNCLASSIFIED	
18. SUPPLEMENTARY NOTES This work sponsored by the Defense Nuclear Agency under RDT&E RMSS Code B323077464 R99QAXEE50207 H2590D.		15a. DECLASSIFICATION/DOWNGRADING SCHEDULE	
19. KEY WORDS (Continue on reverse side if necessary and identify by block number) Prescribed Current Source SGEMP Calculations Dipole Moment Driver			
20. ABSTRACT (Continue on reverse side if necessary and identify by block number) Two limits of applicability of the SGEMP prescribed current source driver, are investigated. The first limit considered occurs when the SGEMP boundary layer thickness is smaller than a cell size. The second limit occurs when a significant number of photoelectrons travel to distances comparable with satellite dimensions during times of interest. Suggestions are made for increasing the effectiveness of prescribed source drivers for the second limit.			

DD FORM 1 JAN 73 1473 EDITION OF 1 NOV 65 IS OBSOLETE

UNCLASSIFIED

SECURITY CLASSIFICATION OF THIS PAGE (When Data Entered)

406 548

slt

CONTENTS

	PAGE
ILLUSTRATIONS	2
SECTION	
1 INTRODUCTION	3
2 CODE MODEL OF P DRIVER	6
3 ANALYTIC MODELS	8
3.1 SKIN CURRENT SOLUTION IN LEGENDRE POLYNOMIALS	9
3.2 POINT DIPOLE	10
4 PHOTOELECTRONS AT LARGE DISTANCES	14
5 SUMMARY OF RESULTS	28
REFERENCES	29

ACCESSION for		
NTIS	White Section	<input checked="" type="checkbox"/>
DOC	Buff Section	<input type="checkbox"/>
UNANNOUNCED		<input type="checkbox"/>
JUSTIFICATION _____		
BY _____		
DISTRIBUTION/AVAILABILITY CODES		
Dist. AVAIL. and/or SPECIAL		
A		

ILLUSTRATIONS

FIGURE		PAGE
1	\bar{G} as a function of δ , $\theta_A = \frac{\pi}{15}$, $\theta_B = \frac{2\pi}{15}$, $\theta_C = \frac{3\pi}{15}$.	16
2	\bar{G} as a function of δ , $\theta_D = \frac{4\pi}{15}$, $\theta_E = \frac{5\pi}{15}$, $\theta_F = \frac{6\pi}{15}$.	17
3	\bar{G} as a function of δ , $\theta_G = \frac{2\pi}{15}$, $\theta_H = \frac{8\pi}{15}$, $\theta_I = \frac{9\pi}{15}$.	18
4	\bar{G} as a function of δ , $\theta_J = \frac{10\pi}{15}$, $\theta_K = \frac{11\pi}{15}$, $\theta_L = \frac{12\pi}{15}$.	19
5	\bar{G} as a function of δ , $\theta_M = \frac{13\pi}{15}$, $\theta_N = \frac{14\pi}{15}$, $\theta_O = \pi$.	20
6	\bar{I} , $\frac{\pi}{15} \leq \theta \leq \frac{3\pi}{15}$.	23
7	\bar{I} , $\frac{4\pi}{15} \leq \theta \leq \frac{6\pi}{15}$.	24
8	\bar{I} , $\frac{7\pi}{15} \leq \theta \leq \frac{9\pi}{15}$.	25
9	\bar{I} , $\frac{10\pi}{15} \leq \theta \leq \frac{12\pi}{15}$.	26
10	\bar{I} , $\frac{13\pi}{15} \leq \theta \leq \frac{14\pi}{15}$.	27

SECTION 1 INTRODUCTION

Analytic models which represent photoelectron currents in SGEMP calculations, are useful for overcoming grid limitations of three-dimensional simulations and also to circumvent the large cost of particle calculations in three or two dimensions. The \dot{P} driver, an analytic model which represents the buildup of the space-charge-limited boundary layer, has been used quite successfully in some code calculations.^{1,2} In other calculations it has not been completely successful.^{3,4} This note examines the applicability of the usual \dot{P} driver, for SGEMP calculations, under two limiting circumstances.

A source current is prescribed in the first spatial grid above the emitting surface in the \dot{P} driver model. This source current represents the total integrated strength of the source currents above the emitting surface. If photoelectrons travel too far from the surface during times of interest or travel very little, relative to grid size in the code, the \dot{P} driver approximations are violated. This note examines the applicability of the usual \dot{P} driver code model when Maxwell-solver spatial grid dimensions, Δx , are larger than the characteristic dimensions of the SGEMP boundary layer, λ_D . In this limit the source region is artificially extended above the surface. An examination of the model is also made under the circumstances that a significant number of particles escape to distances of the order of satellite dimensions during times of interest.

The examinations are made by means of two quasi-static analytic solutions for fields on the surface of a conducting sphere. The sphere is

chosen because the analytic solutions are available or easily obtained; the quasi-static limit is applicable for satellites which are highly damped electromagnetically. The results of the investigation show that if Δx is a large fraction of characteristic body dimensions, R (R is the radius of the sphere, for example), while λ_D is a small fraction of R , the skin currents are in error to first order by approximately $\Delta x/R$. These results suggest, for circumstances where Δx is a significant fraction of body dimensions (but $(\Delta x/R)^2$ can be neglected), that the skin currents generated from a \dot{P} calculation be augmented by a factor like $1 + \beta \Delta x$, where β is, in general, dependent upon position ($\beta = R^{-1}$, for a sphere, far from the source region boundary). Unfortunately for bodies other than a sphere, β is not well defined and most bodies have more than one characteristic dimension. If $(\Delta x/R)^2$ cannot be neglected there is probably no simple correction factor available.

If in the real physical problem a large fraction of particles actually escape the boundary layer, to distances comparable to the satellite dimensions, during times of interest, their consideration may significantly affect the skin current. Modeling these distant currents with a \dot{P} driver alone forces them to contribute to the skin currents as if they were right at the surface, rather than at a distance away from the surface. It is shown, in this note, that the error, in using a \dot{P} driver to model distant photoelectrons, is largest at points on the surface near the source region boundary; the calculated currents will be too large if an accurate \dot{P} calculation is made which includes all the geometrical effects. (These effects reduce the fields which retard photoelectron motion and therefore increase the \dot{P} above that calculated from purely one-dimensional considerations.) To correct for the effect of distant electrons prescribed current sources should be defined in a portion of the space outside the exposed surface, and not just at the exposed surface. A one-dimensional code calculation which includes geometrical effects may still be useful to define these additional prescribed sources. The one-dimensional calculation, alone, will be useful if edge effects can be neglected.

In Section 2 we briefly describe the usual method of incorporating a \dot{P} driver in an SGEMP code calculation. We then examine two quasi-static sphere calculations in Section 3, for $\Delta x > \lambda_D$. In Section 4 we examine the situation in which the effect of photoelectrons at large distances must be considered. The spatial extent over which additional prescribed sources must be defined is also considered. Section 5 is a summary of results.

SECTION 2
CODE MODEL OF \dot{P} DRIVER

The theory of the \dot{P} driver is based upon the assumption that during the times of interest photoelectrons emitted from a continuous electromagnetic surface do not go far from the surface. That is if R is the characteristic dimensions of the emitting surface and $d(t)$ is the distance the majority of electrons have gone in a time t , then \dot{P} is an appropriate driver if

$$R \gg d(t) ,$$

and we are making magnetic field observations at points which are distant (greater than $d(t)$) from discontinuities (corners of an emitting object, for example) in the emission surface. Under these circumstances the error made in treating the spatial photoelectron currents as if they occur only at the emission surface is small ($O(d/R)$). In a finite difference code a current, J_e , equivalent to the spatial distribution of currents is prescribed in the first half cell above the emission surface. The prescription is made by recognizing that the physical quantity which generates time varying fields, for $R > d$, is the time rate of change of dipole moment per unit area \dot{P} . The idea of the code model is to simulate the \dot{P} of the physical problem by setting

$$\Delta x J_e = \dot{P} , \quad (1)$$

where Δx is the grid size perpendicular to the emission surface. This prescription essentially establishes a charge density, whose center is one Δx above the surface, equal to $P(t)/\Delta x$ as a function of time. $\dot{P}(t)$ is obtained by means of a one-dimensional particle calculation. Problems can

arise with this prescription if λ_D/R is negligible when compared to one but $\Delta x/R$ is not, and also when $d(t) \sim R$ during times of interest. The computational model does not, then, correspond to the physical situation. In the next section we investigate the errors generated by this lack of correspondence.

79⁷ 02 05 068

SECTION 3 ANALYTIC MODELS

Taking a sphere as a representative object for SGEMP analysis, we investigate the effect, on skin currents, of radially extended dipole layer sources at the surface. We assume that the actual dipole layer thickness is much smaller than the radius, R , of the sphere and evaluate the error generated when a dipole layer is set up in accordance with Equation 1. According to this prescription, a charge layer is set up a distance Δx from the surface. It is now assumed that $\Delta x/R$ is not negligible.

Reference 5 describes the exact quasi-static analytic solution for skin current generated on a perfectly conducting sphere by spatial currents. This solution is made in terms of an expansion in Legendre polynomials. In Section 3.1 we use this solution to evaluate the error due to a finite $\Delta x/R$. It will be shown that to first order in $\ell\Delta x/R$ the percent error in the magnitude of the ℓ^{th} Legendre coefficient of skin current is $.5\ell \frac{\Delta x}{R}$. The error increases with the order of the solution coefficients and can be large where higher order terms are important.

To obtain a physical understanding of how skin currents can be smaller than expected we consider a second solution, the skin currents on a sphere due to a single point dipole. This solution can be obtained without the use of Legendre polynomials and although the solution is less general it lends itself to greater physical interpretation.

3.1 SKIN CURRENT SOLUTION IN LEGENDRE POLYNOMIALS

Assuming that the spatial currents, $J(r, \theta, t)$, are only in the r direction, substitution of these currents into Equation 24 of Reference 5 gives the equation describing the dependence of the skin current coefficient $K_\ell(t)$ on the Legendre coefficients of the spatial current J_ℓ as

$$K_\ell(t) = - \frac{R^\ell}{\ell} \int_R^\infty J_\ell(r', t) r'^{-\ell} dr' \quad , \quad \ell \geq 1 \quad . \quad (2)$$

In Equation 2, r is the radial coordinate of the spherical coordinate system whose center is at the center of the sphere, (θ is the spherical polar coordinate). The currents are taken to be axisymmetric so the skin current is expanded in Legendre polynomials of order one and J is expanded in Legendre polynomials of order zero. The Legendre coefficients for this latter expansion are J_ℓ . The radius of the sphere is R .

We now assume that $J(r, \theta, t)$ can be represented by

$$\begin{aligned} J(r, \theta, t) &= - \dot{P}/\Delta x h(\theta) f(t) \quad R \leq r \leq \Delta x \\ J(r, \theta, t) &= 0 \quad \Delta x < r < \infty \quad . \end{aligned} \quad (3)$$

Equations 3 are essentially saying that the space-charge layer sets up with the same time history $f(t)$, for any θ , and retarded effects are unimportant ($h(\theta)$ is independent of time). Substituting Equations 3 into 2, after defining $\delta \equiv \Delta x/R$, we find that

$$K_\ell(t) = \frac{\dot{P} \gamma_\ell f(t)}{\ell} \epsilon_\ell(\delta) \quad \ell \geq 2 \quad , \quad (4)$$

$$\epsilon_\ell(\delta) = (1 - (1+\delta)^{-\ell+1}) (\delta^{\ell-1})^{-1} \quad , \quad (5a)$$

$$\epsilon_\ell(\delta) \approx 1 - \frac{\ell\delta}{2} + \ell(\ell+1) \frac{\delta^2}{6} + \theta((\ell\delta)^3) \quad , \quad (5b)$$

and that

$$K_1(t) = P\gamma_1 f(t)\epsilon_1(\delta) , \quad (6)$$

$$\epsilon_1(\delta) = \delta^{-1} \ln(1+\delta) , \quad (7a)$$

$$\approx 1 - \frac{\delta}{2} + \frac{\delta^2}{3} . \quad (7b)$$

In Equations 4 and 6, γ_ℓ are the Legendre expansion coefficients of $h(\theta)$. If $\delta \rightarrow 0$ in Equations 5 and 7 $\epsilon_\ell(\delta) \rightarrow 1$ so that $P\delta_\ell f(t)\ell^{-1}$ is the skin current coefficient for a very thin dipole layer and $\epsilon_\ell(\delta)$ is the fraction of the skin current coefficient observed for an extended dipole. Table 1 calculates $(\epsilon_\ell(\delta))^{-1}$ for $\delta = .3$ from Equations 5a and 7a. ϵ_ℓ^{-1} is the factor that the observed value of skin current coefficient would be multiplied by to obtain the current due to a thin dipole.

Table 1. Correction factor as a function ℓ , $\delta = .3$

ℓ	1	2	3	4	5	6
$(\epsilon_\ell(.3))^{-1}$	1.14	1.30	1.47	1.64	1.85	2.04

Table 1 shows that the error made in extending a small dipole causes the skin current to be too small. It also shows that at those points where a large number of polynomials are necessary to describe the solution (edges, boundaries, etc.) the error is largest.

3.2 POINT DIPOLE

We now consider the skin current on a perfectly conducting sphere due to negative point charge, $-q$, at $\theta = 0$, $r = R + \Delta x \equiv y$. The physical content of this solution is clear and it is general in the sense that a sum of point dipoles can yield a total solution. It is simplest to begin from the expression for the electric field, $\vec{E}(\vec{r}, t)$, in space, finding the charge density and then the surface current. The electric field is

$$\vec{E} = - \frac{q(\vec{r}-\hat{k}y)}{|\vec{r}-\hat{k}y|^3} + \frac{q \frac{R}{y} (\vec{r}-\hat{k} \frac{R^2}{y})}{|\vec{r}-\hat{k} \frac{R^2}{y}|^3} + \frac{q(1 - \frac{R}{y})\hat{r}}{r^2} . \quad (8)$$

We are assuming in Equation 8 that the charge $-q$ was removed from a neutral sphere leaving a charge q on the sphere. The charge density $\sigma(\theta, t)$ on the surface is then easily seen to be, if $e \equiv R/y$

$$\sigma = - q/4\pi R^{-2} [(e^3 - e)(1 + e^2 - 2e \cos \theta)^{-3/2} - 1 + e] . \quad (9)$$

The equation of continuity on the sphere is

$$\frac{1}{R \sin \theta} \frac{\partial}{\partial \theta} (\sin \theta K) = - \frac{\partial \sigma}{\partial t} , \quad (10)$$

where K is the skin current. Substituting (9) into (10), integrating and requiring $K(0) = 0$ we find that the current $I(\theta)$ crossing a circle made by the intersection of the plane $z = R \cos \theta$ and the sphere is

$$\begin{aligned} I(\theta, t) &= 2\pi R \sin \theta K(\theta, t) \\ &= \dot{q}/2(1-e) \left[\frac{1+e}{(1+e^2-2e \cos \theta)^{1/2}} + \cos \theta \right] , \end{aligned} \quad (11)$$

where a dot over q means differentiation with respect to time. Note that at $\theta = 0$, $I(0) = \dot{q}$ or our solution represents the situation in which a thin current exists between the charge at $r = R + \Delta x$, $\theta = 0$ and the surface of the sphere at $\theta = 0$. The magnitude of this current is \dot{q} . Equation 11 will form the basis of the analysis of the effect of distant electrons, in Section 4. In this section we again look at the situation in which $\Delta x > \lambda_D$.

Since we want our solution to correspond to a charge near the sphere we transform the independent variable of Equation 11 from e to δ where

$$\delta \equiv \Delta x/R , \quad (12)$$

and

$$e = (1+\delta)^{-1} , \quad (13)$$

or

$$I(\theta, t) = \dot{\bar{P}}(2R)^{-1} \epsilon(\delta, \theta) \quad (14)$$

where

$$\epsilon(\delta, \theta) \equiv (1+\delta)^{-1} [(2+\delta)(4(1+\delta)\sin^2\theta/2+\delta^2)^{-1/2} + \cos\theta] , \quad (15)$$

and

$$\dot{\bar{P}} \equiv \dot{q}\Delta x . \quad (16)$$

If we assume that δ is small and $\theta > \delta$, then

$$\frac{2 + \delta}{(4(1+\delta)\sin^2\theta/2+\delta^2)^{1/2}} \sim \frac{1}{\sin\theta/2} \left[1 - \frac{\delta^2}{8} (\cot^2\theta/2) \right] , \quad (17)$$

in Equation 15 and

$$\epsilon(\delta, \theta) \approx S(\theta)(1-\delta+\delta^2) - \frac{\delta^2}{8} \frac{\cos^2\theta/2}{\sin^3\theta/2} , \quad (18)$$

where

$$S(\theta) \equiv (\sin\theta/2)^{-1} + \cos\theta . \quad (19)$$

It is clear from Equation 18 that as $\Delta x \rightarrow 0$ (in such a way that $\dot{\bar{P}}$ is finite) the distribution of current on the sphere is given by $I(\theta, t) = (2R)^{-1} \dot{\bar{P}} S(\theta)$. If δ is a significant fraction then the percent error due to a finite Δx is, from Equation 18, just δ itself, to $\theta(\delta^2)$. The δ^2 error term in Equation 18 suggests that the largest percent error will occur for θ near zero (near the dipole position). Table 2 shows values of $S(\theta)/\epsilon(\theta, \delta)$, computed from Equations 15 and 19, for $\delta = .3$, at various θ , to illustrate the difference between currents due to a dipole of negligible length and those due to a dipole of finite length.

Table 2. Correction factor for finite length dipole, $\delta = .3$.

	$\frac{\pi}{32}$	$\frac{\pi}{16}$	$\frac{\pi}{8}$	$\frac{\pi}{4}$	$\frac{3\pi}{8}$	$\frac{\pi}{2}$	$\frac{5\pi}{8}$	$\frac{3}{4} \pi$	$\frac{7}{8} \pi$	π
$S(\theta)/\epsilon(\theta, .3)$	3.39	2.04	1.51	1.34	1.32	1.31	1.30	1.31	1.30	1

$S(\theta)/\epsilon(\theta, \sigma)$ is the factor the currents generated by the finite dipole should be multiplied by to obtain the current due to dipole of negligible length. Table 2 substantiates the suggestion that the error due to a finite dipole length is largest near the dipole ($\theta \leq \Delta x/R$) and about $\Delta x/R$ for most of the region where $\Delta x/R > \theta$. If the sphere were excited by a distribution of dipoles Δx could correspond to a finite grid size; outside the source region the error due to approximating a negligibly thin dipole layer by one of finite size would then be $\Delta x/R$, neglecting terms of $\theta(\Delta x/R)^2$.

SECTION 4
PHOTOELECTRONS AT LARGE DISTANCES

In this section we investigate the errors involved in computing skin currents by means of a \dot{P} driver when the condition $R \gg d(t)$, discussed in Section 2, is not satisfied. To accomplish the investigation we analyze how currents in space, at various distances from the surface of a sphere, contribute to the skin current on that sphere. Letting $\dot{q} \rightarrow \frac{\partial}{\partial t} \bar{\sigma}(r,t)dr$ in Equation 11, where $\bar{\sigma}$ is a charge per unit length, we can, by means of the equation of continuity and an integration by parts, show that

$$I(\theta, t) \equiv \int_0^{\infty} J(x, t) \frac{\partial}{\partial x} G(x, \theta) dx, \quad (20)$$

where

$$G(x, \theta) = \frac{1}{2} \delta(1+\delta)^{-1} \left(\frac{2 + \delta}{(4(1+\delta) \sin^2 \frac{\theta}{2} + \delta^2)^{1/2}} + \cos\theta \right), \quad (21)$$

G in Equation 21 is just $\epsilon(\delta, \theta)$ in Equation 15 multiplied by $1/2$; δ is now x/R , however, and x is the distance of the source current from the surface of the sphere. We can easily show, from Equation 21, that

$$\frac{\partial G}{\partial x} \equiv \frac{1}{2R} \bar{G} = \frac{1}{2R} \left[\frac{\beta}{(1+\delta)^2} + \frac{\delta^3(2\alpha-1) + \delta^2(6\alpha) + \delta(12\alpha) + 8\alpha}{(1+\delta)^2(\delta^2 + \delta(4\alpha) + 4\alpha)^{3/2}} \right] \quad (22)$$

where

$$\beta \equiv \cos\theta, \quad (23)$$

$$\alpha \equiv \sin^2 \frac{\theta}{2}. \quad (24)$$

Figures 1 through 5 are plots of \bar{G} as a function of δ for various θ from 0 to π and indicate how effective spatial currents are in producing surface currents. Figures 1 through 5 demonstrate that an infinitesimal current source close to the surface of the sphere ($\delta = 0$) are much more effective in producing currents near the source boundary (the source is at $\theta = 0$) than far from it. This is no surprise. When the source current is placed farther from the sphere it becomes ineffective in producing currents near the source but less ineffective in producing currents farther from the source; in Figure 1, for example \bar{G} at $\delta = .5$ is greatest for $\theta = 3\pi/15$ and smallest for $\theta = \pi/15$. As θ increases the change in effectiveness of a source current as it is placed further from the sphere decreases. These results are consistent with those of Section 3.

At any angle however a source current is more effective near the surface than farther from it. In other words assuming that all the emission current is placed at $\delta = 0$, as in the \dot{P} model ($\dot{P} = \int_0^\infty J dx$)—whereas in fact it is distributed in space—causes an overestimate to be made in the magnitude of the skin current at any point on the sphere surface. Calculations³ showing a \dot{P} prescribed current source model giving too small a result occur because \dot{P} , calculated from purely one-dimensional considerations is too small or edge effects* are important. Reference 3 suggests that the electric fields, in the vicinity of the source region, which retard the photoelectrons motion away from the surface, are reduced by skin currents. This reduction allows more electrons to get farther from the surface increasing \dot{P} . To first order the reduction in the force on the photoelectron is given by a factor of $1 - b \frac{\lambda_D}{R}$ for this later (the skin current effect) effect where b is a constant. The reduction of the force on the electron due to the decrease of force with

* By edge effect we mean spatial currents which are basically two-dimensional in nature and are caused by electrons escaping the system from an edge or by electrons which are emitted near the edge of the source region but return to an unilluminated portion of the satellite. Edge effects are not considered in this note.

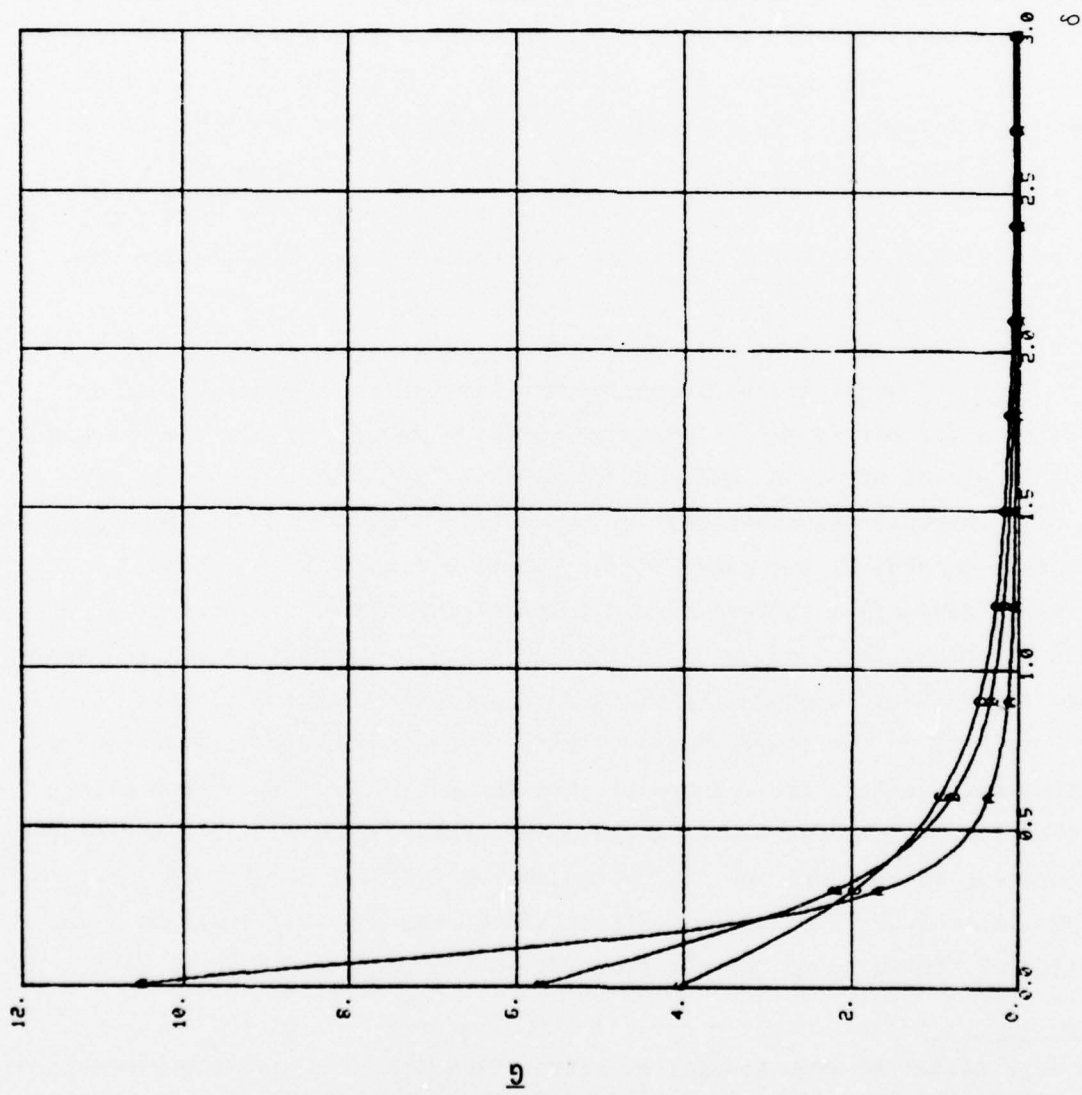


Figure 1. \bar{G} as a function of δ , $\theta_A = \frac{\pi}{15}$, $\theta_B = \frac{2\pi}{15}$, $\theta_C = \frac{3\pi}{15}$.

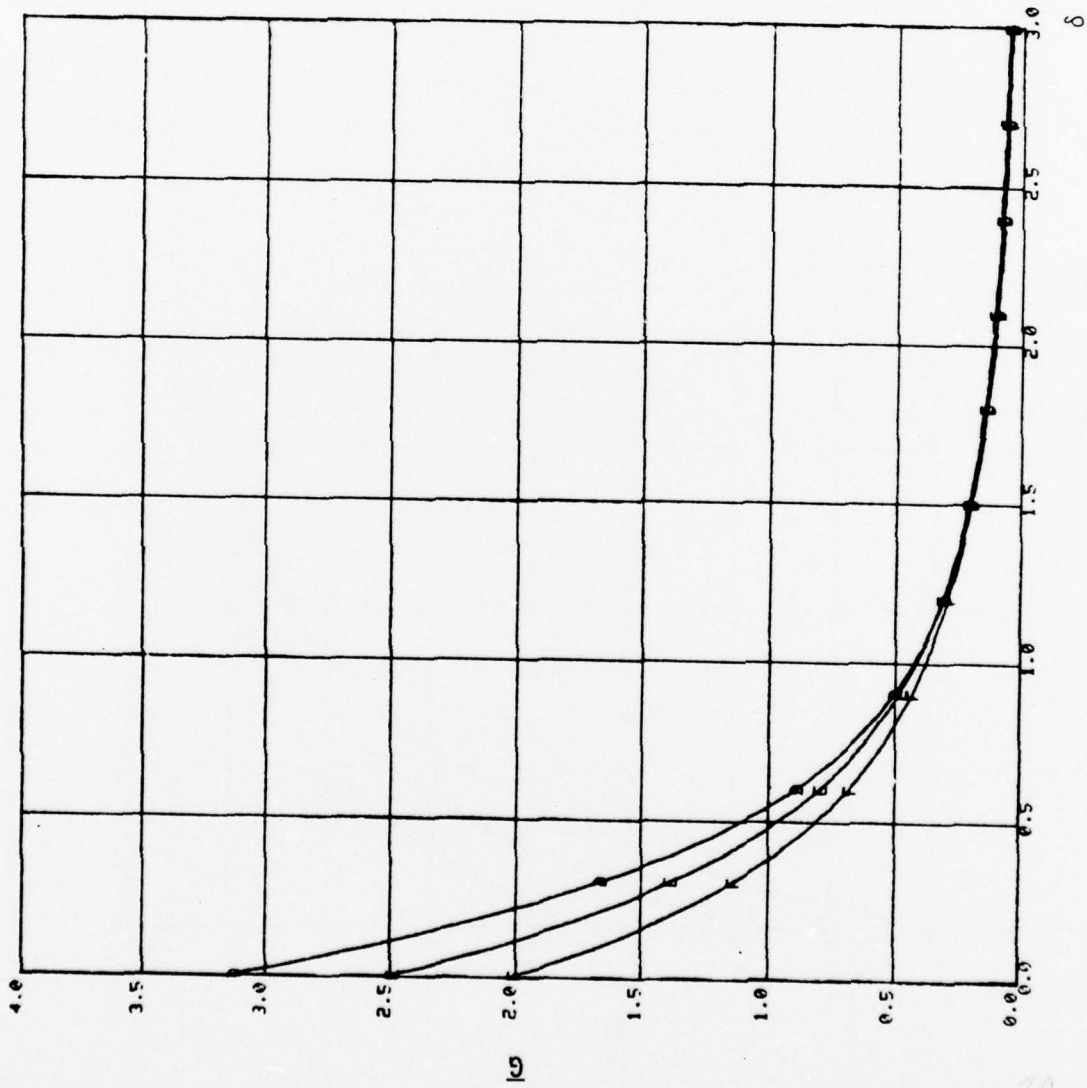


Figure 2. \bar{G} as a function of δ , $\theta_D = \frac{4\pi}{15}$, $\theta_E = \frac{5\pi}{15}$, $\theta_F = \frac{6\pi}{15}$.

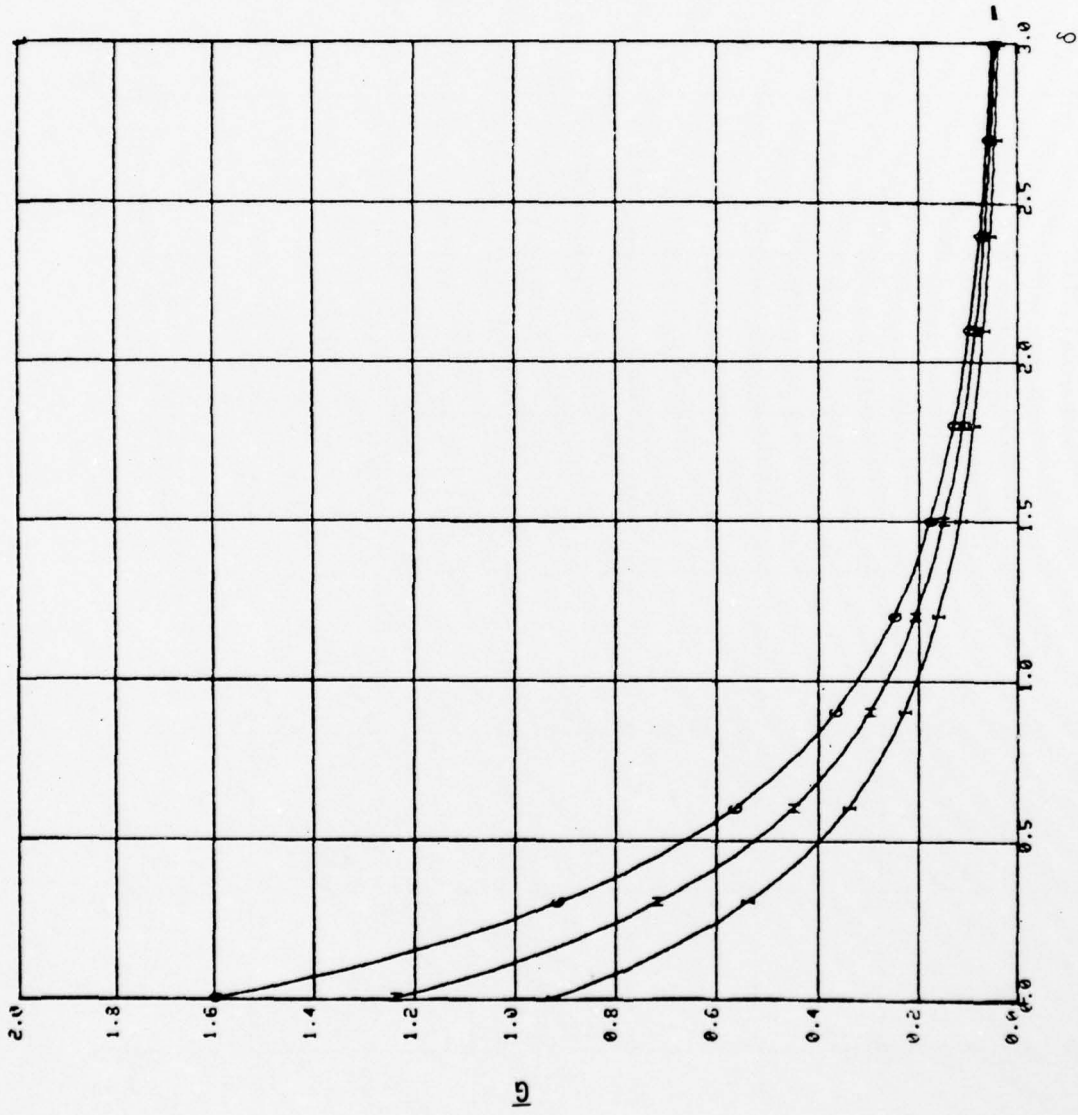


Figure 3. \bar{G} as a function of δ , $\theta_G = \frac{2\pi}{15}$, $\theta_H = \frac{8\pi}{15}$, $\theta_I = \frac{9\pi}{15}$.

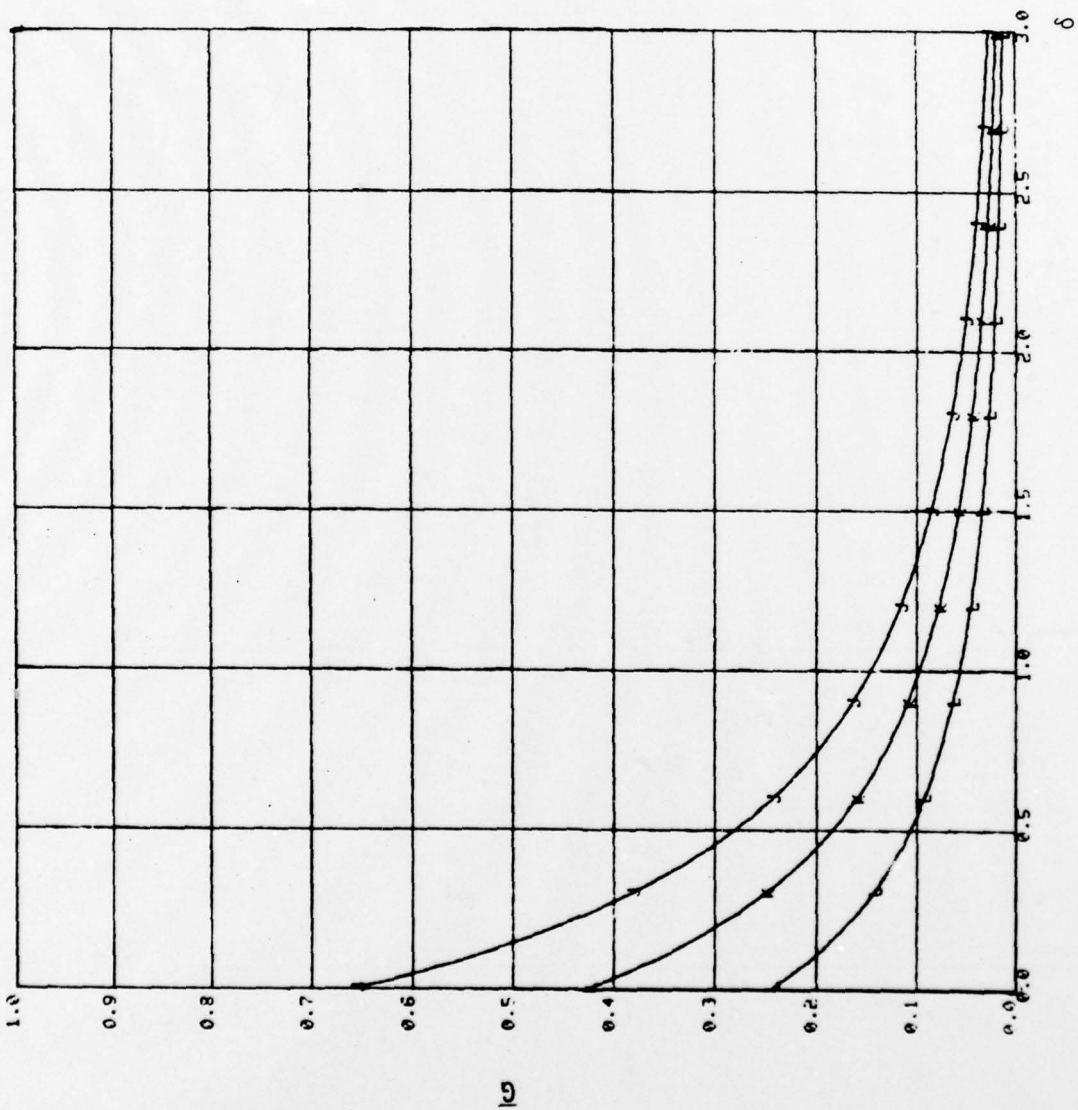


Figure 4. \bar{G} as a function of δ , $\theta_J = \frac{10\pi}{15}$, $\theta_K = \frac{11\pi}{15}$, $\theta_L = \frac{12\pi}{15}$.

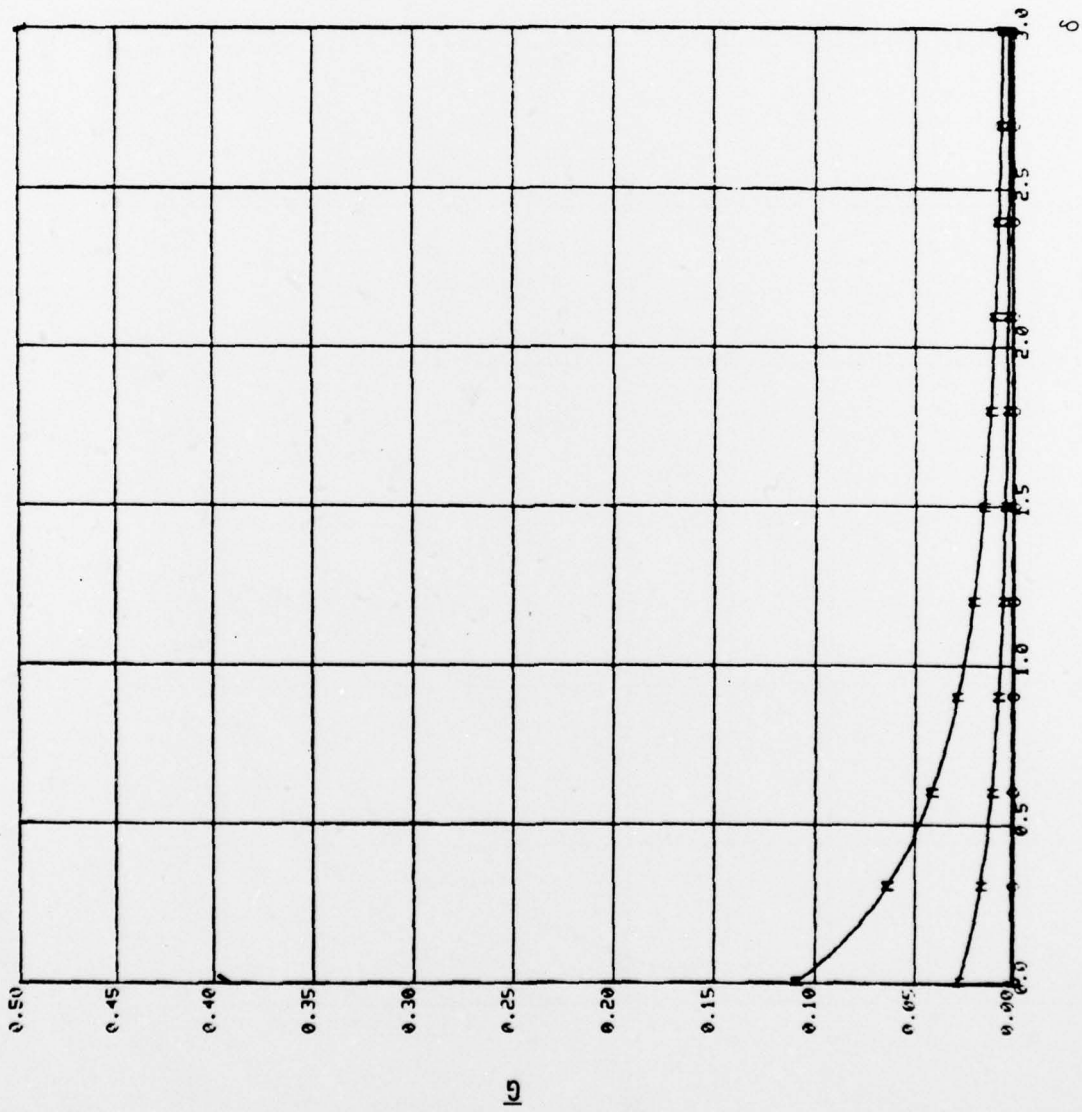


Figure 5. \bar{G} as a function of δ , $\theta_M = \frac{13\pi}{15}$, $\theta_N = \frac{14\pi}{15}$, $\theta_0 = \pi$.

distance from a finite body is also of the order $\frac{\lambda_D}{R}$. Most likely neglecting both these effects contribute to the error in \dot{P} . Calculating \dot{P} by means of a one-dimensional code in spherical or cylindrical coordinates would give a more accurate \dot{P} . It has also been suggested that the skin current effect could be incorporated into the one-dimensional calculation^{*,6} allowing an even more accurate calculation of \dot{P} to be available, in those cases where electrons do travel an appreciable fraction of the satellite dimensions ($\frac{\lambda_D}{R}$ not small), during the times of interest.

Figures 1 through 5 indicate, however, that if particles do move far from the surface and \dot{P} now accurately represents the real \dot{P} the skin currents calculated by a \dot{P} model will be too large. An effective way to compensate for the overestimate is to prescribe currents in the space above the emission surface as well as at the surface. These additional spatial currents could be obtained, just as the original \dot{P} model was obtained, by running a one dimension calculation. The one-dimensional calculation would be more sophisticated only in as much as the geometrical effects, as described above, were included in the calculation.

To obtain some idea of how far in space the currents should be prescribed, Equation 20 was integrated for a simple spatial variation. The spatial current, J , was constant for $0 \leq x \leq \infty$. We denote the skin current caused by the spatial current from $0 < x < x'$ by $I(\theta, x')$, where from Equation 20 and 22 (dropping the t)

$$I(\theta, x') = (2R)^{-1} \int_0^{x'} J(x) \bar{G} dx, \quad (25)$$

and we also define

* B. Goplen did incorporate the skin current effect for the special case of a cylinder (Reference 3), into a one-dimensional calculation. The results suggest that this effect may be correct for the discrepancy between a particle pushing and a \dot{P} simulation of the problem for the radiated field.

$$\bar{I}(\theta, \delta') \equiv \frac{I(\theta, x')}{I(\theta, \infty)}, \quad (26)$$

where

$$\delta' = x'/R. \quad (27)$$

Figures 6 through 10 are plots of \bar{I} as a function of δ' , for various θ . It is clear from the figures that contributions to the current close to the source (small δ') mainly come from currents close to the surface. At larger values of δ' currents farther from the surface make a stronger contribution to the skin current. The physical situation resulting in Figures 6 through 10 is extreme in that the spatial currents extend all the way to infinity and only a very small portion of the surface is part of the source region. Even in this extreme case the skin current would be in error, by less than 35 percent, if we integrated only up to one radii from the sphere, for most positions on the spherical surface.

Some judgement is necessary in deciding to what extent prescribed currents need to be defined in space in order to perform an accurate SGEMP simulation. Equation 25 and Figures 6 through 10 should be helpful in making these decisions. In most circumstances, where peak skin current is of primary interest, it will probably not be necessary to prescribe the source beyond one characteristic radii of the satellite.

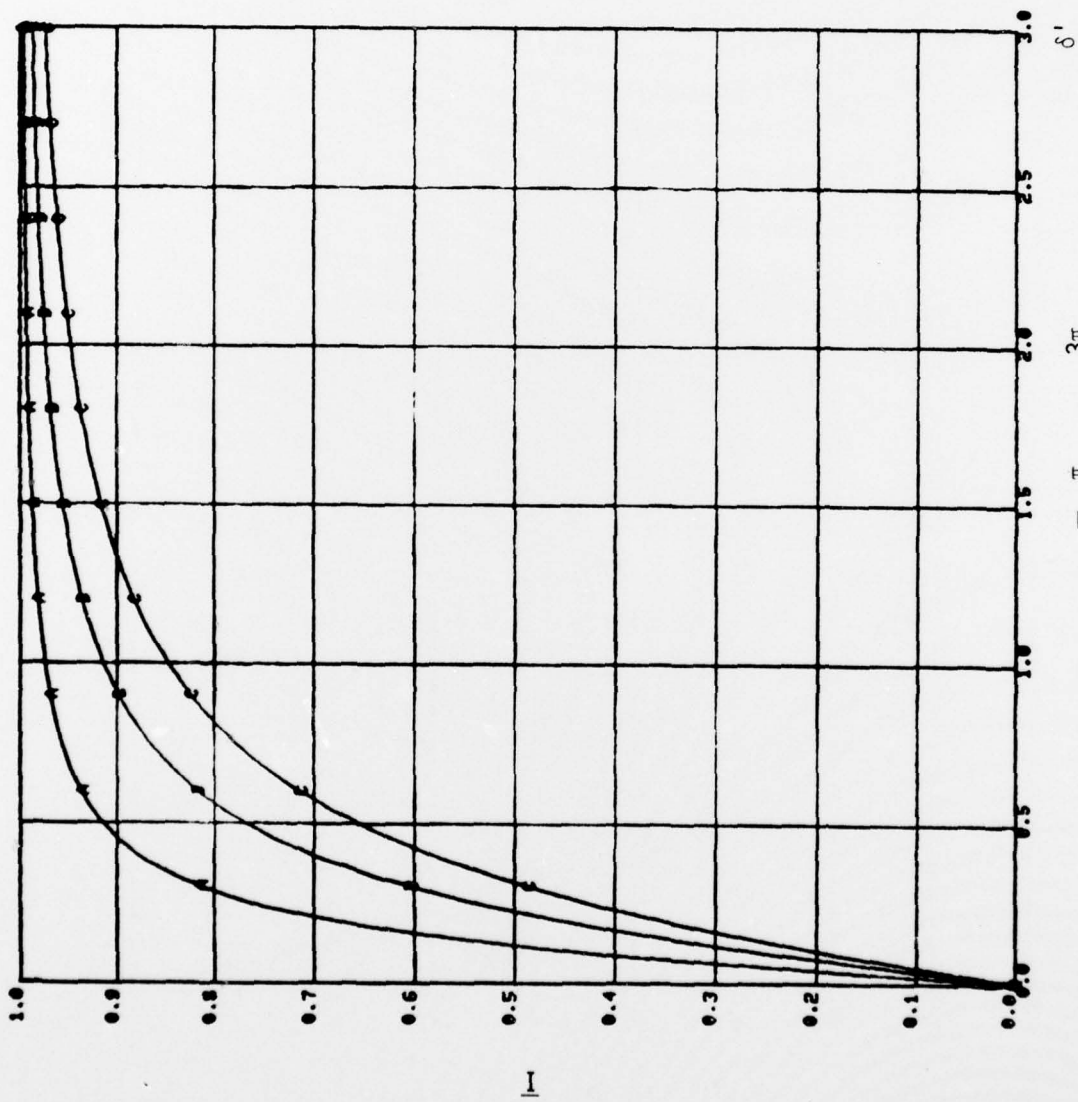


Figure 6. $I, \frac{\pi}{15} \leq \theta \leq \frac{3\pi}{15}$.

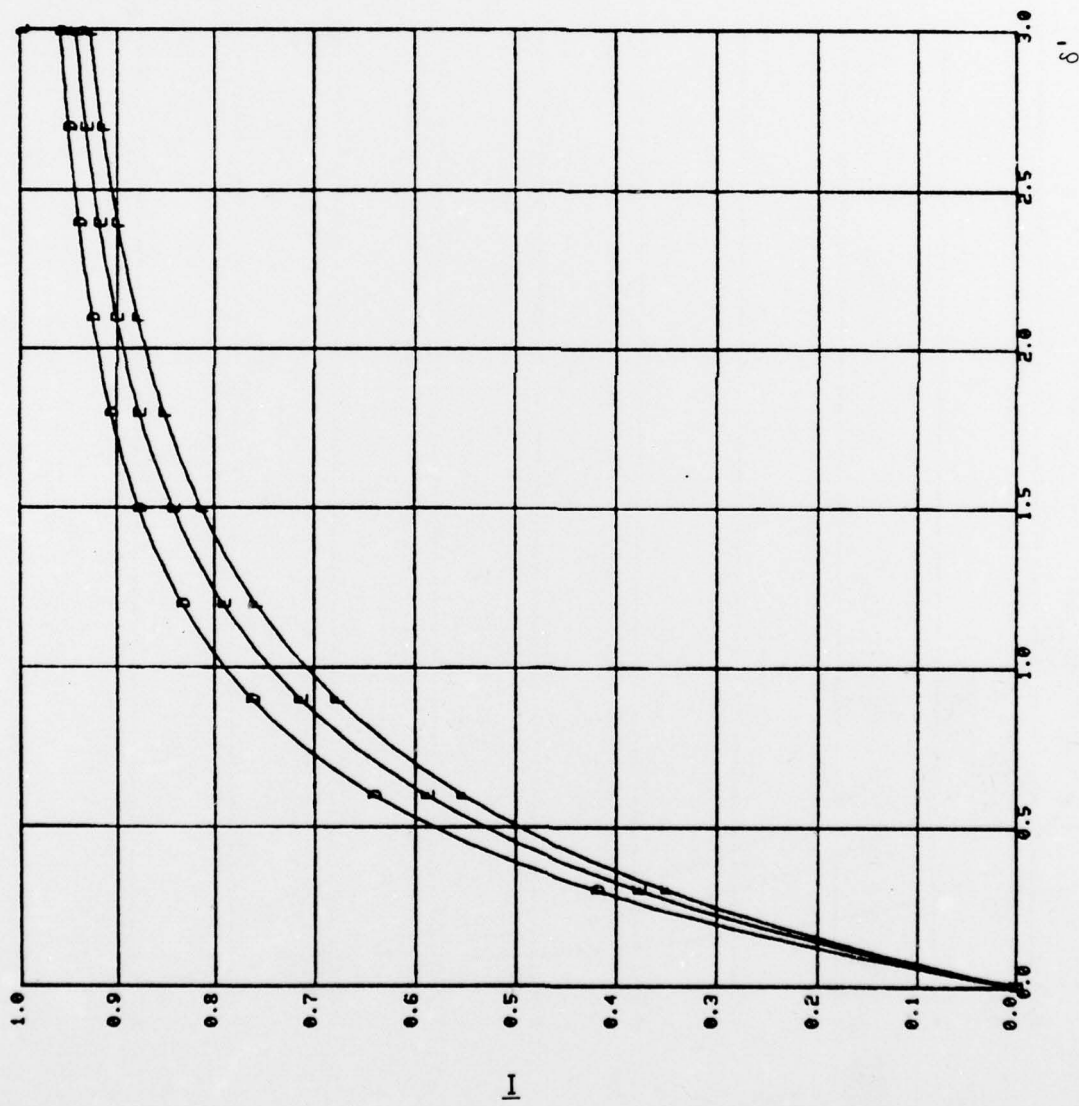


Figure 7. $\frac{4\pi}{15} \leq \theta \leq \frac{6\pi}{15}$.

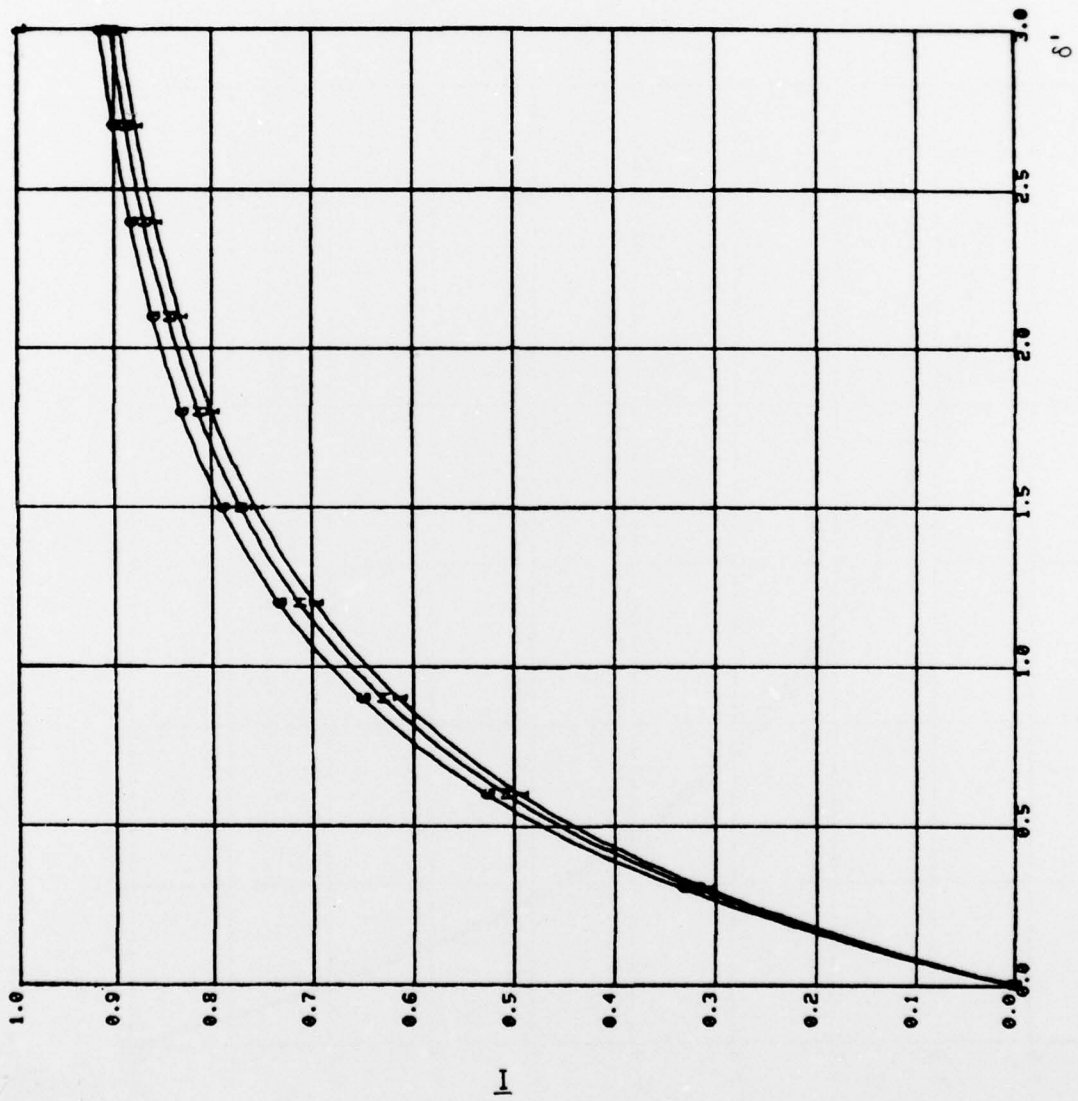


Figure 8. $\bar{I}, \frac{7\pi}{15} \leq \theta \leq \frac{9\pi}{15}$.

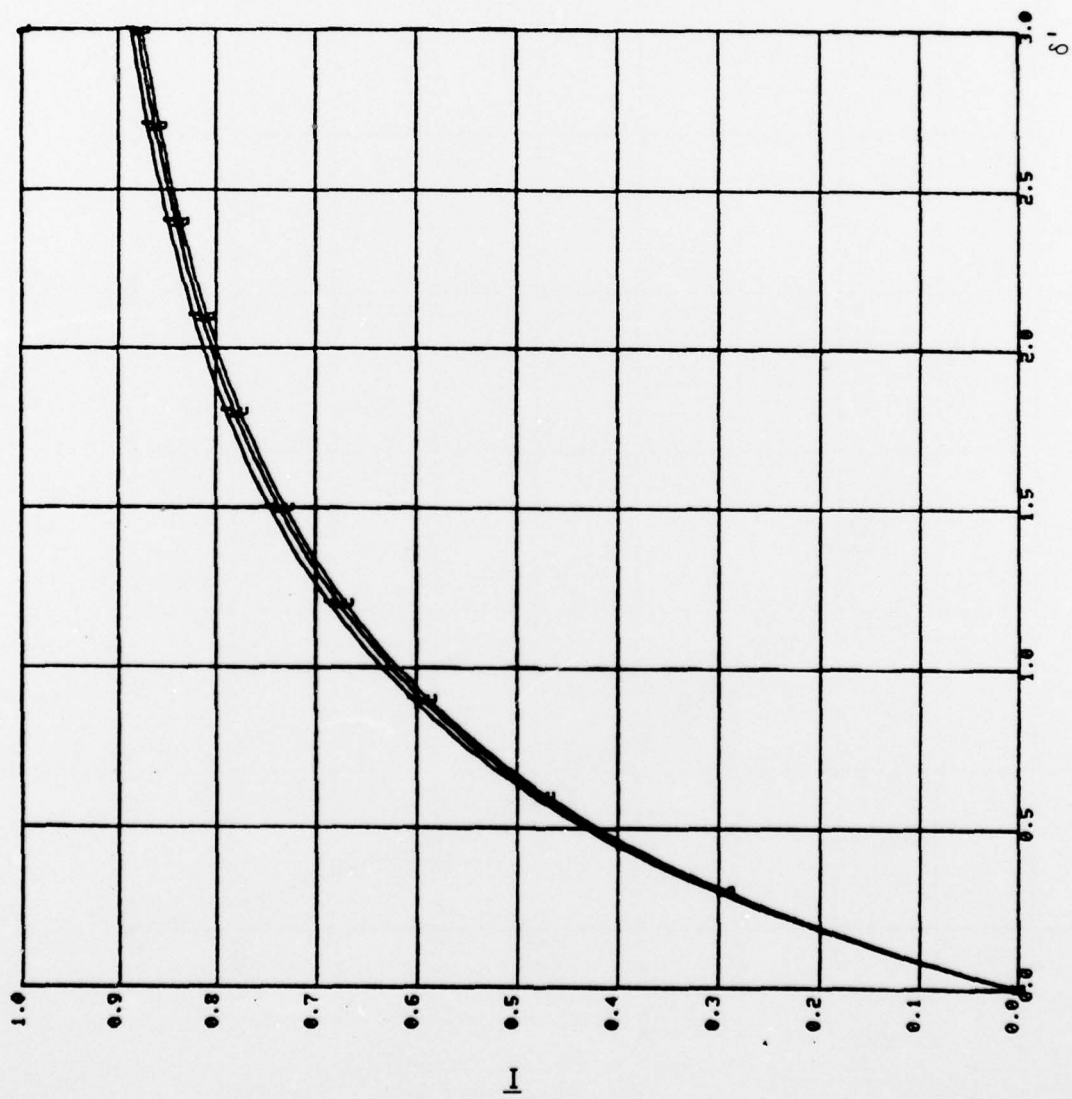


Figure 9. $I, \frac{10\pi}{15} \leq \theta \leq \frac{12\pi}{15}$.

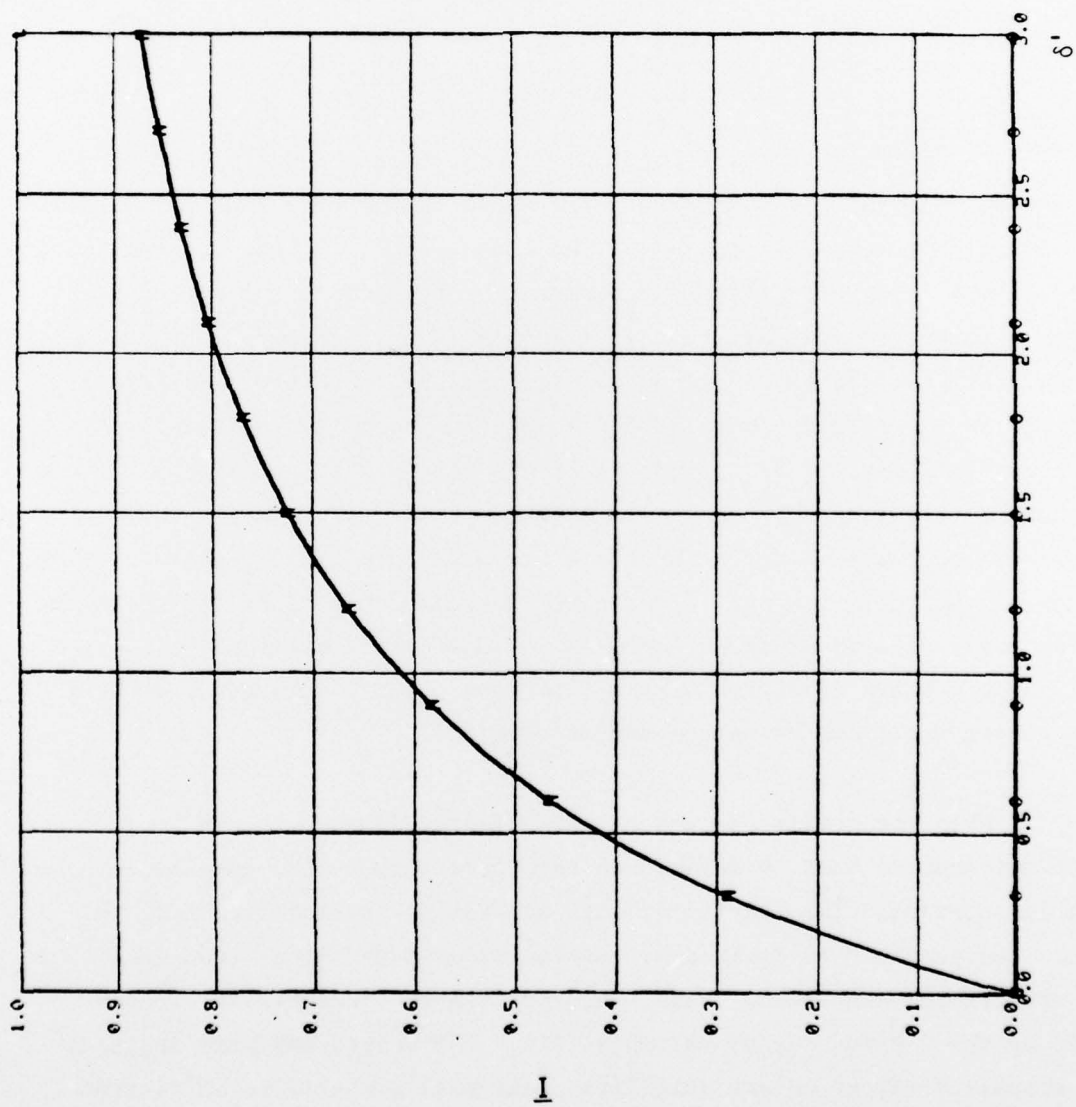


Figure 10. $I, \frac{13\pi}{15} \leq \theta \leq \frac{14\pi}{15}$.

SECTION 5 SUMMARY OF RESULTS

An analysis of the limitations of the \dot{P} driver was made using a quasi-static analysis of a sphere. Errors are caused by either artificially over extending the spatial region of the photoelectron source current or not really taking into account the large extent of the source current region. Figures 1 through 5 indicate that if a source is over extended the calculated skin currents will be too small, as in the case $\Delta x > \lambda_D$ (Δx is the spatial grid size in a multidimensional SGEMP Maxwell solver). In contrast, if a source current consists of distant electrons and they are treated as though they are all near the surface the calculated skin currents will be too large. To accurately account for the error made when $\Delta x > \lambda_D$ would require, in general, an understanding of the electromagnetic nature of the satellite but the error will be of the order $\Delta x/R$, if $(\Delta x/R)^2$ is negligible, where R is a characteristic dimension of the satellite. For a sphere the error is exactly $\Delta x/R$ far from the source region boundary.

When the spatial extent of the affective source region is large, prescribed sources must be defined in the space outside the satellite as well as at the surface. The spatial extent, as well as the magnitudes of the sources can probably be defined by running a one-dimensional code (assuming edge effects are negligible) which incorporates the geometrical effects caused by the finite size of the satellite. The sphere analysis suggests that a spatial extent of one satellite radii will probably be sufficient for most situations in which peak skin currents are sought.

REFERENCES

1. Crevier, W. J., James L. Gilbert, R. Macgurn, and R. Marks, AFWL OWL Exploding Wire Exposure: MRC Post Shot Predictions, MRC-R-323, Mission Research Corporation, May 20, 1977.
2. Stettner, R., V. A. J. van Lint, D. Fromme, and B. Goldstein, Research in SGEMP, Volume II—Response of Simple Geometries, MRC-R-367, Mission Research Corporation, January 1978.
3. Goplen, B., A Comparison of Four Treatments of Space-Charge-Limiting, SAI-77-511-AQ, Science Applications, Inc., December 1977.
4. van Lint, V. A. J., D. A. Fromme, R. Stettner, M. L. Price and M. Van Blaricum, Research in SGEMP, Volume IV—RESMOD, MRC-SD-R-367, Mission Research Corporation, January 20, 1978.
5. Stettner, R., and D. F. Higgins, X-ray Induced Currents on the Surface of a Metallic Sphere, MRC-N-111, DNA 3612T, Mission Research Corporation, April 1975.
6. Crevier, W., J. Gilbert, and B. Goplen, private communication.

DISTRIBUTION LIST

DEPARTMENT OF DEFENSE

Armed Forces Staff College
ATTN: Reference & Technical Services Branch

Assistant Secretary of Defense
Program Analysis and Evaluation
ATTN: Dep. Assist Sec. (Strategic Programs)
ATTN: Dir. Special Weapons & Support Systems Div.

Defense Advanced Rsch. Proj. Agency
ATTN: Director
ATTN: TIO

Defense Civil Preparedness Agency
Assistant Director for Research
ATTN: Staff Dir. Rsch., G. Sisson

Defense Documentation Center
12 cy ATTN: DD

Defense Intelligence Agency
ATTN: DT-1B, E. Decker
ATTN: DT, J. Vorona
ATTN: DB-4C, E. O'Farrell
ATTN: DT-1, M. Fletcher

Defense Nuclear Agency
4 cy ATTN: TITL
ATTN: DDST
ATTN: RAEV

Field Command
Defense Nuclear Agency
ATTN: FCPR

Joint Chiefs of Staff
ATTN: J-3, E. Burkhalter
ATTN: J-5, R. Lawson

Livermore Division, Field Command, DNA
Lawrence Livermore Laboratory
ATTN: FCPRL

National Defense University
ATTN: Classified Library

National Security Agency
Department of Defense
ATTN: D9, J. Amato

Office of the Under Secretary of Defense
Assistant for Analysis
ATTN: Director

Secretary of Defense
ATTN: Special Assistant

Under Secretary of Defense for Rsch. & Engrg.
ATTN: Strategic & Space Systems (OS)
ATTN: Strategic & Space Systems

DEPARTMENT OF THE ARMY

Deputy Chief of Staff for Ops. & Plans
Department of the Army
ATTN: E. Meyer

Harry Diamond Laboratories
Department of the Army
ATTN: DELHD-N-TD, W. Carter
ATTN: DELHD-N-NP

U.S. Army Materiel Dev. & Readiness Cmd.
ATTN: Commander

U.S. Army Nuclear & Chemical Agency
ATTN: Library

U.S. Army War College
ATTN: Library

DEPARTMENT OF THE NAVY

Naval Surface Weapons Center
ATTN: Code F31

Naval War College
ATTN: Code E-11

Nuclear Weapons Plans Policy and Reg. Br.
Plans Policy and Operations, OCNO
ATTN: NSP-10

Office of the Chief of Naval Operations
ATTN: Op-009
ATTN: Op-02
ATTN: Op-09, R. Long
ATTN: Op-03
ATTN: Op-090
ATTN: Op-05

DEPARTMENT OF THE AIR FORCE

Aerospace Defense Command
ATTN: Commander

Air Force Institute of Technology, Air University
ATTN: Library

Air Force Office of Scientific Research
ATTN: NA, B. Wolfson

Air Force Systems Command
ATTN: DL

Air Force Weapons Laboratory
ATTN: SUL
ATTN: DYC

Air University Library
Department of the Air Force
ATTN: AUL-LSE-70-250

DEPARTMENT OF THE AIR FORCE (Continued)

Assistant Chief of Staff
Intelligence
Department of the Air Force
ATTN: INA

Deputy Chief of Staff
Operations Plans and Readiness
Department of the Air Force
ATTN: AFX00
ATTN: AFX0X
ATTN: AFX0

Deputy Chief of Staff
Research, Development, and Acq.
Department of the Air Force
ATTN: AFRDQ
ATTN: AFRD
ATTN: AFRDQSM

Deputy Chief of Staff
Programs and Analyses
Department of the Air Force
ATTN: PAC, J. Welch, Jr.

Foreign Technology Division, AFSC
ATTN: NIIS, Library
ATTN: SDBS, J. Pumphrey

Space & Missile Systems Organization/CC
Air Force Systems Command
ATTN: CC

Space & Missile Systems Organization/MN
Air Force Systems Command
ATTN: MN MGen Hepfer

Space & Missile Systems Organization/RS
Air Force Systems Command
ATTN: RS, L. Norris

Strategic Air Command/XPFS
Department of the Air Force
ATTN: DCS/Plans

DEPARTMENT OF ENERGY

Department of Energy
ATTN: D. Kerr

Department of Energy
ATTN: J. Dentsch

Office of Military Application
Department of Energy
ATTN: Doc. Con. for Gen Bratton

OTHER GOVERNMENT AGENCY

Central Intelligence Agency
ATTN: RD/SI, Rm. 5G48, Hq. Bldg. for OSR

DEPARTMENT OF DEFENSE CONTRACTORS

Abington Corporation
ATTN: J. Weiss

Aerospace Corporation
ATTN: W. Mann

DEPARTMENT OF DEFENSE CONTRACTORS (Continued)

Avco Research & Systems Group
ATTN: J. Stevens

BDM Corporation
ATTN: J. Braddock

Boeing Company
ATTN: D. Isbell

Brookhaven National Laboratory
Technical Support Org. for Safeguard
ATTN: J. Indusi

R. E. Dougherty
ATTN: R. Dougherty

G. A. Kent
ATTN: G. Kent

General Electric Company
Re-Entry and Environmental Systems Div.
ATTN: C. Raver

General Electric Company
Washington Office
ATTN: Dr. Rodgers
ATTN: R. Minckler

General Electric Company-TEMPO
Center for Advanced Studies
ATTN: DASIAC

General Research Corporation
Santa Barbara Division
ATTN: Technical Information Office

Henry S. Rowen
ATTN: H. Rowen

Hercules, Inc.
ATTN: Library

Institute for Defense Analyses
ATTN: J. Bengston

JAYCOR
ATTN: E. Wenaas

Kaman Sciences Corporation
ATTN: A. Bridges

Lawrence Livermore Laboratory
University of California
ATTN: Doc. Con. for Dr. Batzel
ATTN: Doc. Con. for L-38, H. Reynolds
ATTN: Doc. Con. for L-203, L. Germain

Lockheed Missiles and Space Company, Inc.,
ATTN: Document Control

MIT Lincoln Lab.
ATTN: L. Loughlin

University of Miami
ATTN: Director of Security for F. Kohler

DEPARTMENT OF DEFENSE CONTRACTORS (Continued)

Mission Research Corporation
ATTN: R. Stettner
5 cy ATTN: Document Control

Northrop Corporation
ATTN: D. Hicks

Pacific-Sierra Research Corporation
ATTN: F. Thomas

PAN Heuristics
Div. of Science Applications, Inc.
ATTN: A. Wohlstetter

R & D Associates
ATTN: C. MacDonald

Rockwell International Corp.
ATTN: N. Rudy

Sandia Laboratories
Livermore Laboratory
ATTN: Doc. Con. for T. Cook

Sandia Laboratories
ATTN: Doc. Con. for Director
ATTN: Doc. Con. for Org. 5000
ATTN: Doc. Con. for R. Peurifoy

DEPARTMENT OF DEFENSE CONTRACTORS (Continued)

Santa Fe Corporation
10 cy ATTN: D. Paolucci

Science Applications, Inc.
ATTN: J. Martin

Systems, Science & Software, Inc.
ATTN: Document Control

TRW Defense and Space Sys. Group
ATTN: R. Chevington

TRW Defense and Space Sys. Group
San Bernardino Operations
ATTN: J. Gorman